

Original article

## Method for Measuring the Dispersion of Capillary Wave Slopes on the Sea Surface

V. V. Sterlyadkin ✉, K. V. Kulikovskiy, M. V. Likhacheva

*MIREA - Russian Technological University, Moscow, Russian Federation*

✉ [sterlyadkin@mail.ru](mailto:sterlyadkin@mail.ru)

### Abstract

**Purpose.** The purpose of this study is to substantiate and practically apply a new method for fast (0.01 s) recording of capillary wave parameters under natural conditions.

**Methods and Results.** The method is based on recording an image of a thin laser beam incidence on the sea surface. The radiation scattered in the water is refracted at the rough interface and is recorded by a video camera located at the side. The beam image deviations are proportional to the surface slopes at the point of radiation exit. The largest slopes, exceeding  $30^\circ$ , are characteristic of capillary waves; this makes the method particularly effective for recording them. It has become possible to record waves with an amplitude of  $30\ \mu\text{m}$  from a distance of 5–8 m. When intense capillary ripples occur below the point of beam incidence on the surface, a light “skirt” is formed, the width of which grows with increasing slope. The distribution of the scattered-light intensity in the cross-section of the light “skirt” makes it possible to calculate the slope distributions for each frame or the probability function for a given time interval. The developed method for the operational determination of the distribution of capillary wave slopes is applied to study the capillary structure of various areas of sea waves, namely the crests and troughs. It is established that the dispersion of capillary slopes in the troughs is significantly lower than that on the crests, which is consistent with previously reported data.

**Conclusions.** A new method for remote measurement of capillary wave slopes on the sea surface is proposed; it permits measurements to be carried out over surface areas of  $10 \times 10\ \text{cm}$  in 0.01 s. The given example shows that at a significant wave height ( $1.1 \pm 0.1\ \text{m}$ ) and a wind speed of ( $7.4 \pm 0.5\ \text{m/s}$ ), the average dispersion of the capillary component was 0.0256 on the crests and 0.008 in the troughs. The advantage of the method is that it makes it possible to carry out measurements in a wide range of weather conditions, both during the night and the day.

**Keywords:** capillary waves, *in situ* measurements, slope distribution, slope dispersion, laser wave recorder

**Acknowledgments:** The study was carried out with the financial support of the Russian Science Foundation, grant No. 23-17-00189 “Investigation of the relationship between the surface wind and the dynamics of wind wave development on the sea surface and the processes of microwave radiation transfer at the sea surface–atmosphere boundary”, <https://rscf.ru/project/23-17-00189/>.

**For citation:** Sterlyadkin, V.V., Kulikovskiy, K.V. and Likhacheva, M.V., 2026. Method for Measuring the Dispersion of Capillary Wave Slopes on the Sea Surface. *Physical Oceanography*, 33(2), pp. 246-262.

© 2026, V. V. Sterlyadkin, K. V. Kulikovskiy, M. V. Likhacheva

© 2026, Physical Oceanography



## Introduction

Capillary waves strongly affect the scattering of electromagnetic waves in the optical and microwave ranges, as well as the intrinsic electromagnetic radiation of the rough sea surface. Although the amplitude of capillary waves usually does not exceed 0.5 mm, their influence on radar backscatter and radiometry is very significant because the slopes of these waves often exceed  $30^\circ$ , leading to increased surface roughness and reflectivity over a wide range of wavelengths [1–4].

Capillary waves have been studied in considerable detail in laboratory tanks, where measurement instruments can be placed in close proximity to the waves [5–9]. However, the parameters of capillary waves in tanks may differ significantly from those of sea waves due to the presence of boundaries and the absence of low-frequency wave components. Recording capillary waves under natural conditions is challenging: measurements must be taken from a distance of 5–10 m for waves with amplitudes of less than 0.5 mm. Additional difficulties arise from the spatial inhomogeneity of capillary waves (their coherence length generally does not exceed 10 cm) and their short lifetime (their coherence time is on the order of tenths of a second).

Methods for measuring slopes from aircraft or satellites based on sun-glint reflection are known [10–12]. However, they require sunlight and favourable illumination geometry, and the averaging area does not allow the study of capillary waves on small surface patches. There are methods for measuring gravity-capillary wave parameters using stereo photography [13, 14] or polarimetric photography [15–17]. The disadvantages of these methods include high requirements for the uniformity of background illumination and the impossibility of measurements at night. Methods based on recording reflected or refracted laser radiation were developed<sup>1</sup> [18], their drawback is the need to place structural elements underwater or at a short distance from the surface, which distorts the wave field or severely limits operating conditions. A patent<sup>2</sup> describes a method that uses a knife-edge laser beam illuminating the surface, with profile recording by a photo or video camera; however, during the exposure time, the surface boundary shifts, reducing the accuracy of wave-profile measurements. In works<sup>3</sup> [19], a method of scanning the sea surface with a laser beam is proposed, allowing reconstruction of the “instantaneous” interface profile along a given scanning trajectory with a spatial resolution of up to 0.5 mm. Field measurements of “instantaneous” profiles and the calculation of the one-dimensional spatial wave spectrum are described in [20]. Laboratory and field measurements of frequency spectra and surface profiles of capillary waves are presented in [21].

---

<sup>1</sup> Zapevalov, A.S., 2008. *Statistical Models of the Sea Surface in Problems of Acoustic and Electromagnetic Radiation Scattering*. Thesis Dr. Phys.-Math. Sci. Sevastopol, 290 p. (in Russian).

<sup>2</sup> Karaev, V.Yu. and Meshkov, E.M., 2012. [*Method for Determining the Angle of Inclination and Wave Height of a Water Surface Relative to Its Equilibrium State*]. Patent RU 2448324 C2. Bull. No. 11, 8 p. (in Russian).

<sup>3</sup> Sterlyadkin, V.V., 2020. [*Scanning Laser Wave Recorder with Registration of “Instantaneous” Surface Shape*]. Patent RU 2749727 C1. Bull. No. 17, 10 p. (in Russian).

The aim of this work is to substantiate and verify a new method for recording sea-wave slopes, including capillary-wave slopes, based on analyzing the image of a laser beam incident vertically downward on the sea surface and recorded from the side of the beam using a video camera. The proposed method allows the determination of the slope distribution of the capillary-wave fraction over surface areas as small as  $10 \times 10$  cm in 0.01 s. The method sensitivity enables the recording of capillary waves with an amplitude of  $30 \mu\text{m}$  from a distance of 5–8 m. Theoretical substantiation and experimental verification of the method were carried out in previous studies [22, 23]. This paper briefly summarizes the main results of those studies and presents new field data on the parameters of capillary waves on different parts of large wind waves, namely, on the crests and in the troughs.

### **Theoretical substantiation and experimental basis of the proposed method**

Works<sup>3</sup> [19] describe a laser wave recorder that allows obtaining an “instantaneous” sea surface profile under field conditions. The measurement principle is based on scanning the sea surface with a thin laser beam directed vertically downward along a given trajectory with a known time law. Synchronization of the scan start with the start of image recording on the video camera matrix, located to the side of the scan line, provides clear registration of the water–air interface on each frame, corresponding to the wave profile along the entire scan trajectory (Fig. 1, *a*). The illumination duration of each pixel on the trajectory is about  $10^{-4}$  s, so the image is not blurred by vertical wave motion; comparison of adjacent frames allows determining the vertical velocity of each surface point. Due to the finite scan speed, different points on the trajectory are illuminated at different times, so the recorded profile image is not “instantaneous”. However, it can be corrected and reduced to an “instantaneous” form, e.g., to the start of exposure, taking into account the illumination delay for each profile point and its vertical velocity obtained from adjacent frames. The synchronisation accuracy is  $10^{-4}$  s, and the error in estimating wave elevations is determined by the pixel scale and is typically 0.5–1.0 mm.

From 5–10 min video recordings, series of tens of thousands of sea-surface profiles  $\zeta(x, y, t_i)$  can be obtained, as well as the frequency spectrum of waves [19], the slopes  $\xi_x, \xi_y$  along orthogonal axes, and two-dimensional slope distributions  $P(\xi_x, \xi_y)$  at three arbitrary points on the surface (Fig. 1, *b*) can be calculated. The scale of the triangle can be chosen, thereby making it possible to include different scales of wind waves in the analysis. Fig. 1, *b* shows an example of a slope distribution obtained on 21 August 2021 at 20:29 Moscow time on the oceanographic platform of Marine Hydrophysical Institute of Russian Academy of Sciences (MHI RAS). In the center, the scan speed is four times lower than at the edges.

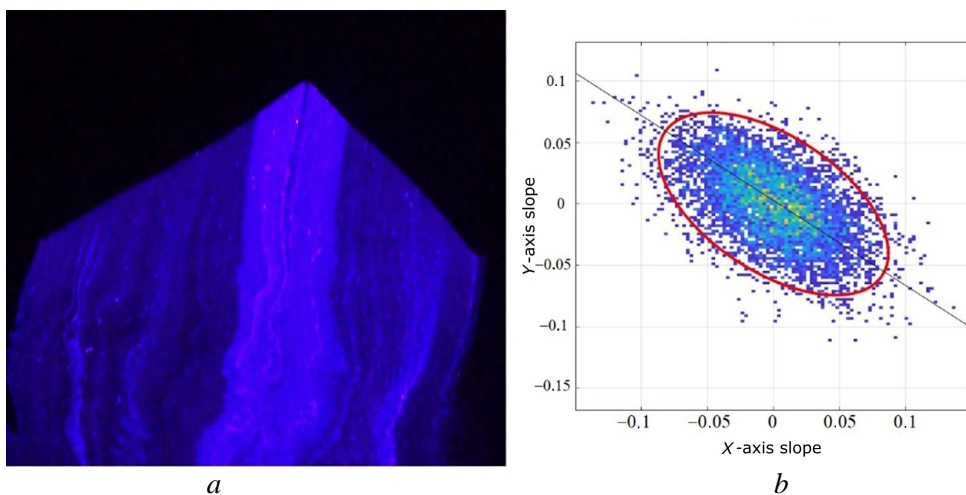


**Fig. 1.** Video frame of laser scanning in two orthogonal directions (*a*); two-dimensional distribution of slopes  $P(\xi_x, \xi_y)$  on a right triangle measuring  $300 \times 300$  mm (*b*)

If the scan trajectory has stops at given points, images of the beam boundaries are formed with a higher signal-to-noise ratio, allowing measurements even during the daytime (Fig. 2).

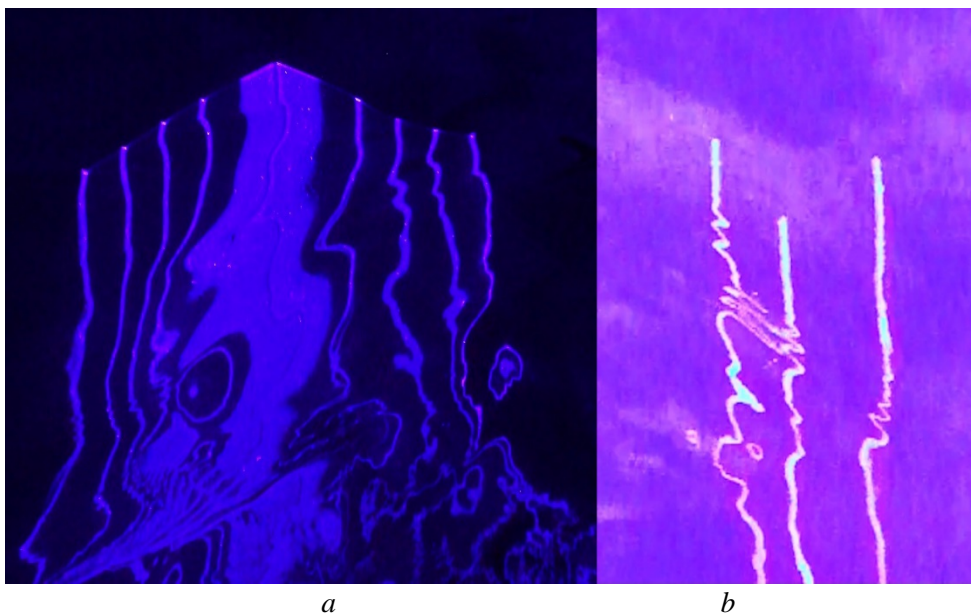


**Fig. 2.** Image of a set of laser beams distorted by a rough surface and formed in water during scanning with stops at specified points (*a*); capillary comb (*b*)

When analyzing video frames, the authors noted that images of laser beams often have a complex shape: arcs, loops, and combs. A thin laser beam incident on the sea surface propagates in water along a straight path and glows due to scattering

by water inhomogeneities. However, the image of the straight beam, when recorded by a video camera located to the side of the incidence point, passes through the rough sea surface and becomes distorted. These distortions depend on the surface slopes at the points of refraction. In [22], a mathematical formulation is given, and an analysis of the inverse problem of reconstructing the sea surface profile from the image of refracted laser beams is carried out. It is shown that, in general, it is impossible to reconstruct the surface profile from a single video frame because the number of unknowns exceeds the number of equations obtained from the laws of refraction by one.

However, when capillary waves appear on the sea surface, a capillary comb often appears on the video frame (Fig. 2, *b*). From the spacing and orientation of such a comb, the magnitude and direction of the wave vector  $\bar{k}$  of the capillary wave, as well as its amplitude, can be determined [23]. Information about the direction of the wave vector provides an additional equation, which allows the inverse problem to be solved and the shape of the capillary wave to be uniquely reconstructed. The correctness of determining capillary-wave parameters from the video image of a straight line has been confirmed in a laboratory experiment [23].

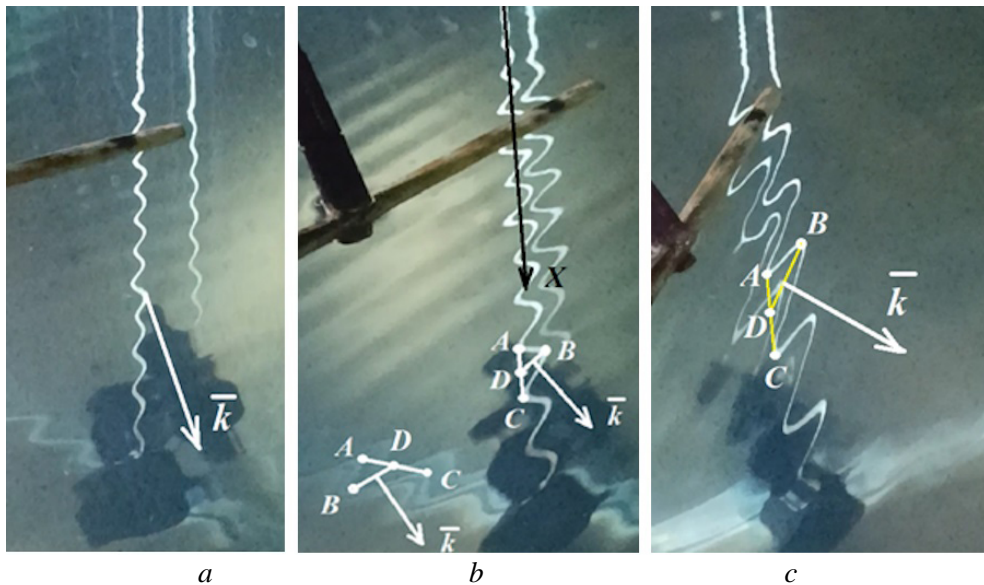


**Fig. 3.** Dependence of the image of a straight white thread (and its reflection from the aquarium wall) distorted by a capillary wave on the surface on the angle  $\theta$  between the wave vector  $\bar{k}$  and the  $X$ -axis of the video camera, with  $\theta$  equal to  $20^\circ$  (*a*),  $40^\circ$  (*b*) and  $55^\circ$  (*c*).  $\triangle ABC$  is a triangle constructed using the points of maximum deviation of the beam image from the undisturbed state;  $BD$  is the median of triangle  $ABC$ . Below is the image of the light lower horizontal edge of the aquarium [23]

Fig. 3 represents images of a vertical white thread obtained when observing the thread through a capillary wave on the surface of an aquarium at different observation angles relative to the vector  $\bar{k}$ . It is shown that the wave vector  $\bar{k}$  is perpendicular to the median

$BD$  of triangle  $ABC$ . The sensitivity of the method based on analyzing the shape of laser beams makes it possible to record capillary waves with an amplitude of  $30\ \mu\text{m}$  under field conditions from a distance of 5–8 m.

In [22], the relationship between the sea-surface slopes  $\xi_x$ ,  $\xi_y$  and the position  $(x, y)$  of the luminous point on the sea surface relative to the point  $(x, y) = (0, 0)$  of laser-beam incidence on the surface was calculated for a specific camera geometry. The camera height above the surface was  $H = 4.70$  m, and the horizontal distance from the beam-incidence point to the projection of the video camera onto the surface was  $L = 6.99$  m. It was revealed that surface slopes  $\xi_x$  in the direction of the camera axis ( $X$  axis) primarily lead to a shift in the image of the luminous point along the luminous beam ( $X$  axis), thus weakly affecting the deviation of the beam image along the  $Y$  axis (perpendicular to the  $X$  axis). Preliminary estimates indicate that this effect does not exceed 16% under the most intense capillary slopes along the  $X$  axis. In contrast, slopes  $\xi_y$  along the orthogonal  $Y$  axis cause a strong deviation of the beam image from the undisturbed line in the  $y$  coordinate. Fig. 4 shows the calculated dependence of the  $y$  coordinate of the luminous point on the slope  $\xi_y$  for the given measurement geometry at  $x_0 = 160$  mm and  $\xi_x = 0$  (the mean slope along the  $X$  axis). The correctness of solving the nonlinear system of equations is confirmed by direct substitution of the solution into the equations of geometric optics.

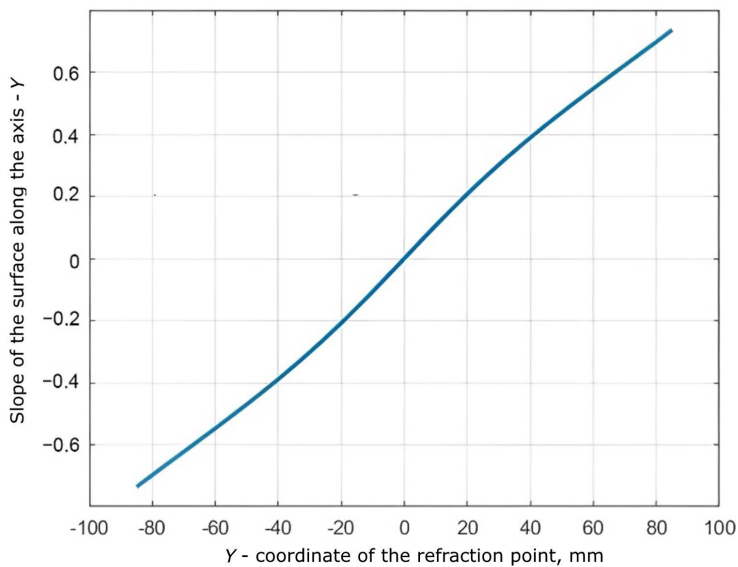


**Fig. 4.** Dependence of the sea-surface slope  $\xi_y(y)$  on the  $y$  coordinate in the luminous point for the described observation geometry at a distance of  $x = 160$  mm from the point of beam incidence on the surface. The slope  $\xi_x$  is taken to be zero

The dependence  $\xi_y(y)$  is monotonic and unambiguous: the farther the luminous point is from the undisturbed position,  $y = 0$ , the greater the sea-surface slope at that point. We will use this dependence to calculate the probability density of sea-surface slopes from video images of the laser beam.

**The light “skirt” method allows the acquisition of an “instantaneous” slope distribution.** Under strong capillary waves, a light “skirt” forms on video frames below the point where the beam enters the water (Fig. 5). Three consecutive video frames were taken at a frame rate of 90 frames per second, with a shutter speed of 1/100 s, wind speed  $V_w$  of 7–8 m/s, significant wave height of  $(1.1 \pm 0.1)$  m, and a spectral peak wave period of  $(7.2 \pm 0.1)$  s. The sea surface was partially covered with capillary ripples. The measurements were carried out on 22 February 2025 at 02:55 Moscow time on the oceanographic platform of MHI RAS.

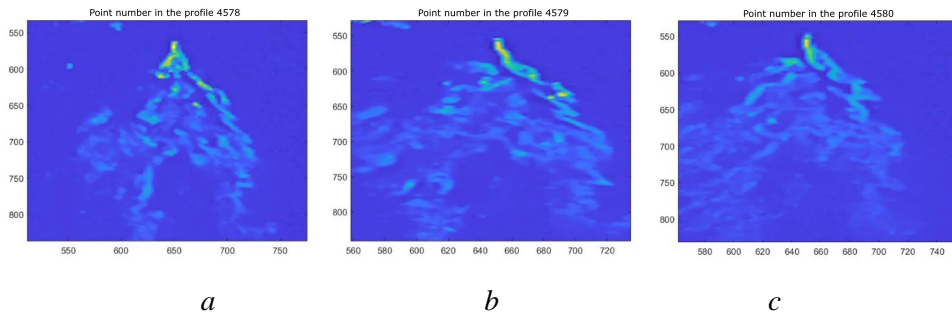


**Fig. 5.** Three consecutive frames: 4578 (*a*), 4579 (*b*) and 4580 (*c*) recorded with a shutter speed of 1/100 s at a video frame rate of 90 frames per second

The appearance of a light “skirt” instead of a laser beam is explained by the fact that capillary waves have frequencies  $\nu$  exceeding 16 Hz; therefore, during the exposure time  $\Delta t = 1/100$  s, the phase of the capillary wave changes by  $2\pi\nu\Delta t$  (by more than 1 rad). The higher the frequency of the capillary wave, the greater the range over which the surface slopes vary at each point. At the same time, at many points on the surface, slopes arise for a short time such that the point begins to glow, i.e. refract the luminous laser beam toward the video camera. The brighter the glow of a given point on the video frame, the larger the fraction of time during which that point has the corresponding slope. Since during one frame the conditions for glowing do not occur at all points where the capillary wave passes, there are areas on a single frame that do not glow. As a result, the light “skirt” appears perforated and “lacey”. The intensity distribution in frame 4578 (see Fig. 5, *a*) along line 715 is demonstrated in Fig. 6.

The intensity distribution (Fig. 6) has a pronounced periodicity associated with the periodicity of capillary slopes on the surface. For a sinusoidal wave, the same slopes repeat twice per period, so two periods in the figure correspond to a periodicity of the capillary structure of  $\Lambda \approx 16$  mm. Considering that the periodicity  $\Lambda$  is recorded along the  $Y$  axis, and that this periodicity is related to the capillary wavelength  $\lambda$  by the relation  $\Lambda = \lambda/\cos(\theta)$ , where  $\theta$  is the angle of deviation of the wave vector  $\bar{k}$  from the  $Y$  axis, we obtain a capillary wavelength  $\lambda$  of less than 16 mm.

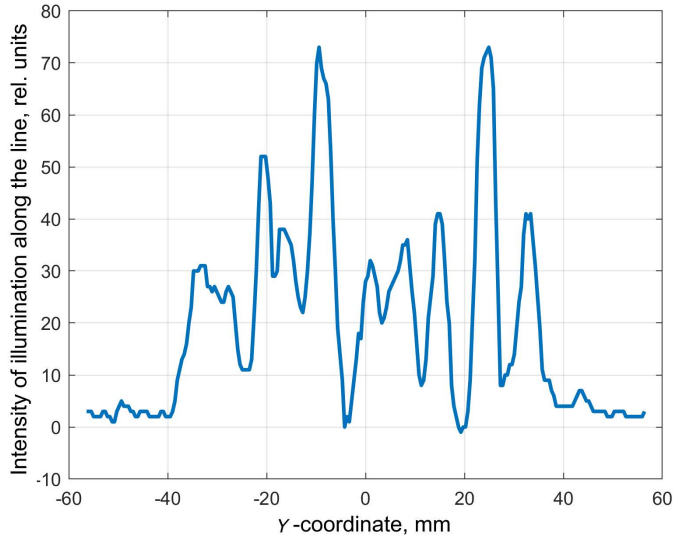


**Fig. 6.** Distribution of the glow intensity of the light “skirt” along line 715 of frame 4578 shown in Fig. 5, *a*

When summing several frames, the glowing areas shift with the wave and overlap, forming a more uniform intensity distribution of the “skirt” glow. If nine frames are summed, the total accumulation time is 0.1 s. During this time, at each point on the surface where a wave with a frequency above 10 Hz passes, the wave phase changes by  $2\pi$  or more, so the slopes also vary over the entire range of values characteristic of that capillary wave. The “skirt” becomes illuminated everywhere the capillary wave is present, and its width is greater for waves with larger maximum slopes.

We now consider the relationship between the brightness distribution of the “skirt” and the surface slopes. For a fixed value of the coordinate  $x_0 = 160$  mm, the dependence of the sea surface slope  $\xi_y(y)$  on the  $y$  coordinate of the luminous point is calculated (see Fig. 4). The light energy falling on the interval  $(y, y + dy)$  is  $I(x_0, y)dy$ , which should be proportional to the probability of the slope falling into the corresponding interval  $P(\xi_y)dy$ , where  $P(\xi_y)$  is the probability density of slopes. Taking into account the relation  $\xi_y(y)$ , we obtain

$$P(\xi_y) = AI(x_0, y) \frac{dy}{d\xi_y}, \quad (1)$$

where  $A$  is a normalization coefficient determined from the condition

$$\int P(\xi_y) d\xi_y = 1. \quad (2)$$

Information about capillary slopes is contained not only in a single line at  $x_0$ , but also in all other lines of the light “skirt”. We now consider the procedure for using information from the entire frame and accumulating information by analysing the intensity distribution of the “skirt” not along one specific line, but across all lines.

Calculations performed using the method described in [22] demonstrate that, for the same surface slope, the displacement of the luminous point along the y coordinate is proportional to the distance x (Fig. 7).

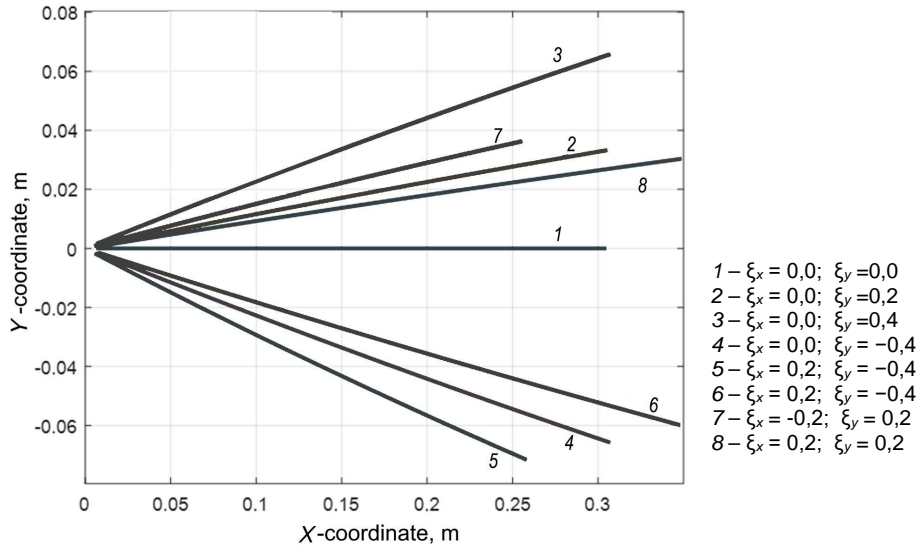


**Fig. 7.** Dependence of the beam displacement along the y coordinate on the distance x at a given surface slope

A consequence of this fact is that the “skirt” shape in the presence of an intense capillary fraction often has the form of a cone starting from the point where the beam enters the water. An example is provided by the frames in Fig. 5. The linear nature of the  $y(x)$  relationship allows all lines to be summed and the entire image to be reduced to one line at  $x_0 = 160$  mm, or the images to be summed over a given range of lines. To do this, it is necessary to account for the linear change in scale by a factor of  $x/x_0$  and the decrease in glow intensity by a factor of  $x/x_0$  due to the distribution of light energy over a different coordinate interval (we neglect the attenuation of radiation when considering a small surface area). Let  $I(x_0, y)$  be the intensity distribution of illumination along the y axis for a given  $x_0$ , and  $I(x, y)$  be the intensity distribution for  $x$  different from  $x_0$ . The normalization procedure for a line with coordinate  $x$  to a single value  $x_0$  can be written as

$$I_n(x_0, y) = \frac{x}{x_0} I\left(x, \frac{x_0}{x} y\right).$$

The normalized intensity distributions are then averaged over a given interval of values  $x_1 < x < x_2$ :

$$I_{av}(x_0, y) = \frac{1}{(x_2 - x_1)} \sum_{x_1}^{x_2} \frac{x}{x_0} I\left(x, \frac{x_0}{x} y\right).$$

It is advisable to choose the averaging interval so that it is neither too close to the beam-incidence point, because pixel saturation may occur near the beginning of the beam, nor too far from it, because in the lower lines of the image the signal-to-background ratio decreases and attenuation of laser radiation in water must be taken into account. Fig. 8, *a, c* shows examples of light “skirts” accumulated over nine frames, and Fig. 8, *b, d* demonstrates the corresponding slope distributions obtained using formulas (1) and (2) with  $I_{av}(x_0, y)$  taken as  $I(x_0, y)$ , averaged over the interval between  $x_1 = 50$  mm and  $x_2 = 160$  mm.

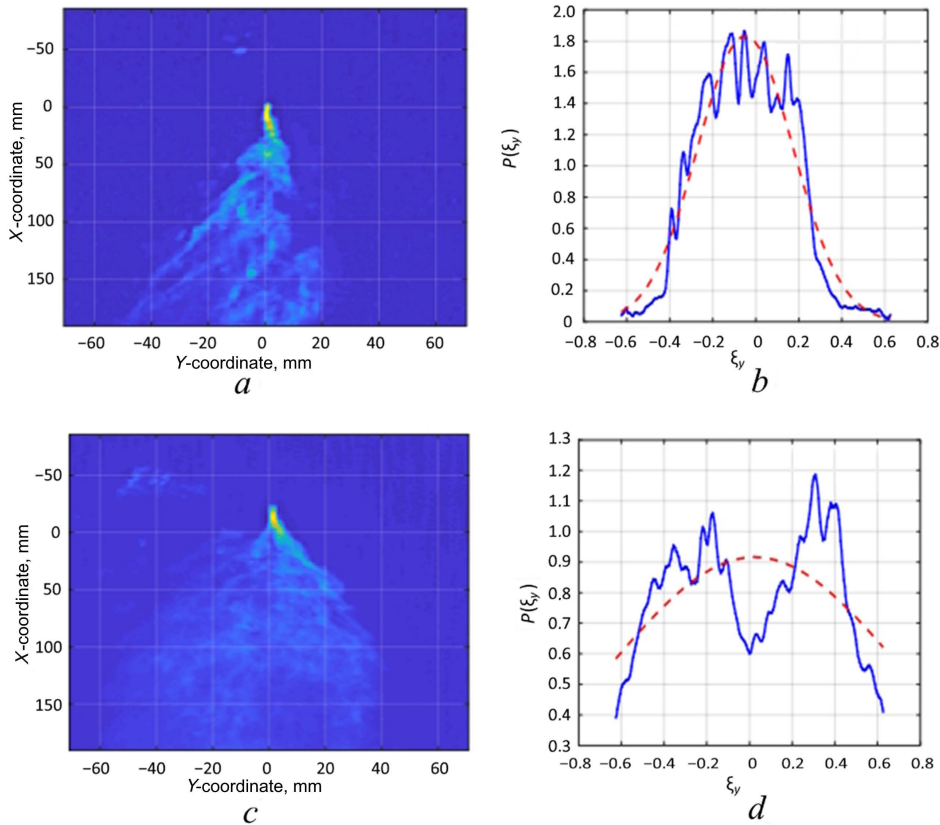


**Fig. 8.** Examples of light “skirts” accumulated over nine frames: from frames 3272 to 3280 (*a*) and from frames 4577 to 4585 (*c*), and the corresponding slope distributions (solid line) with a Gaussian distribution approximation (dashed line) (*b, d*)

In Fig. 8, *b* the slope distribution is shifted from the centre by an average of  $-0.1$ , which characterises the mean slope of the gravity wave over the averaging area. The laser “skirt” is associated with the presence of capillary waves with a root-mean-square (RMS) slope  $\xi_y$  of about  $0.25$ . In Fig. 8, *c* the “skirt” is very wide. The slopes there reach  $0.6$ , which corresponds to an inclination angle of  $34^\circ$ .

Thus, the proposed method for analyzing laser “skirts” makes it possible to obtain an almost “instantaneous” distribution of capillary wave slopes over small ( $100 \times 100$  mm) areas of the sea surface.

## Results

### Structure of capillary waves on crests and in troughs of gravity waves

As an example, we consider measurements carried out on 22 February 2025 at 02:55 Moscow time on the oceanographic platform of MHI RAS. The interface height versus frame number (elevations) of the sea surface at the point of incidence of continuous laser radiation is given in Fig. 9. The video frame rate was 90 frames per second, with a shutter speed of 1/100 s, a video sequence length of 26,000 frames, a significant wave height of  $(1.1 \pm 0.1)$  m, and a wind speed of  $(7.4 \pm 0.5)$  m/s. The wind direction was easterly, with a deviation of  $12^\circ$  from the  $Y$  axis. In the figure, rectangles highlight four sections on wave crests and three sections in troughs, selected for comparing slope dispersions.

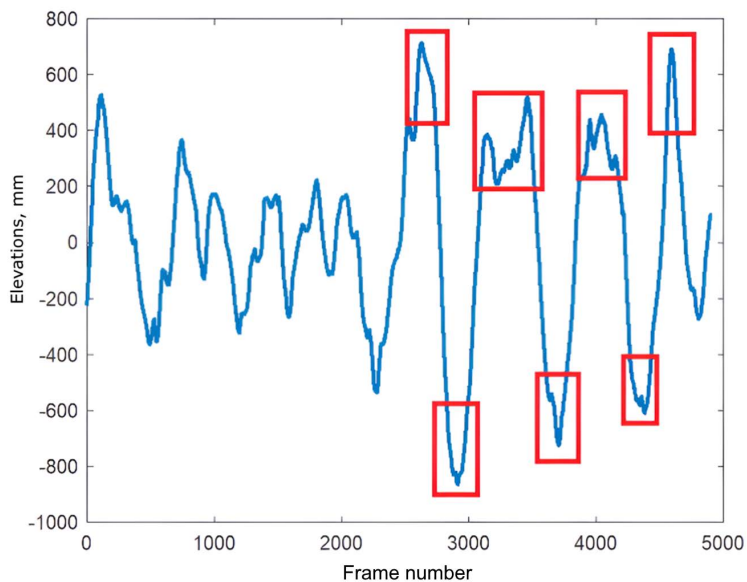


**Fig. 9.** Applicates depending on the frame number. Rectangles denote the analyzed areas

Each section was divided into groups of nine frames, corresponding to an averaging time of 0.1 s, and the images were summed with the incidence point shifted to the origin. Over 0.1 s, gravity slopes change insignificantly, whereas the phase of capillary waves at each point undergoes a full cycle from 0 to  $2\pi$ , ensuring registration of the entire range of capillary slopes. A light “skirt” is then formed. Fig. 10 (top) shows the summed “skirts” obtained in troughs in the frame interval from 3680 to 3706. The corresponding slope distributions are given below in the same figure. Similar data are given in Fig. 11 for crests in the frame interval from 2618 to 2653. The width of the “skirts” on the gravity-wave crest is noticeably larger. The red dashed line on all slope distributions indicates the approximation of the distribution by a normal law.

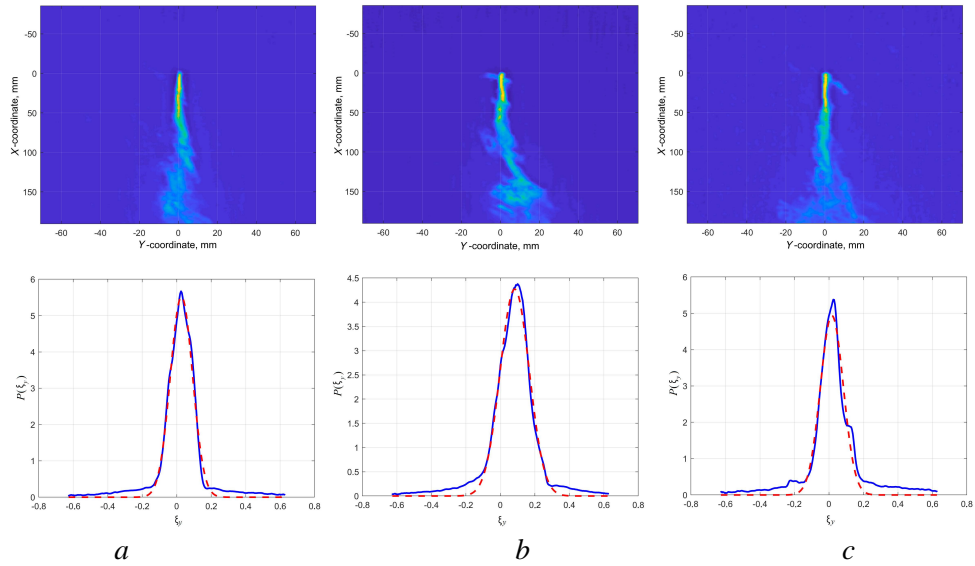


**Fig. 10.** Accumulation of the beam images for 0.1 s (nine frames) in the trough area (in the frame interval 3680–3706 in Fig. 9) (*top*); corresponding slope distributions (*bottom*): *a* – frames 3680–3688; *b* – 3689–3697; *c* – 3698–3706

In a first approximation, the intensity of capillary waves can be estimated by the dispersion  $\sigma_{\xi_y}^2$  of the slope distribution. For a series of four “skirts” in the trough (Fig. 10), the averaged RMS slope  $\sigma_{\xi_y}$  was 0.07 (dispersion 0.0049). A similar value for a series of four “skirts” on the crest (Fig. 11) gave an RMS slope of capillary waves  $\sigma_{\xi_y} = 0.20$ . Averaging over 1/3 of the most pronounced crests and troughs from the 5 min video recording yielded values  $\sigma_{\xi_y}^{\text{tr}} = 0.09$  and  $\sigma_{\xi_y}^{\text{cr}} = 0.16$ . The averaging sample consisted of 98 crests and 94 troughs.

The period of the dominant spectral waves was 7.2 s, and the amplitude was 0.55 m. Since the direction of the  $Y$  axis, along which the slopes are measured, differed from the wind direction (and the direction of long waves) by only  $12^\circ$ , with  $\cos 12^\circ = 0.98$ , we can assume the condition  $k_y = k$ . The Modulation Transfer Function (MTF) is estimated from the obtained data; by analogy with [24, 25], it can be introduced for the modulation of the RMS slope of capillary waves in the form

$$\sigma_{\xi_y} = \overline{\sigma_{\xi_y}} [1 + M \cdot \varepsilon \cdot \sin(\phi - \phi_0)],$$

where  $\overline{\sigma_{\xi_y}}$  is the surface-averaged value of  $\sigma_{\xi_y}$ ;  $M$  is the MTF;  $\varepsilon = kA$  is the steepness of the modulating wave with elevations  $\zeta(y, t) = A \cdot \sin(ky - \Omega t - \phi_0)$ ,  $k = 2\pi/\lambda$  is the wavenumber for long waves propagating along the  $y$  axis,  $A$  is their amplitude, and  $\phi_0$  is the phase shift between  $\zeta$  and  $\sigma_{\xi_y}$ . Given the obtained values, the steepness of the modulating wave  $\varepsilon$  is 0.044, and the obtained RMS slope values of 0.09 and 0.16 are achieved with an MTF of 6.6.

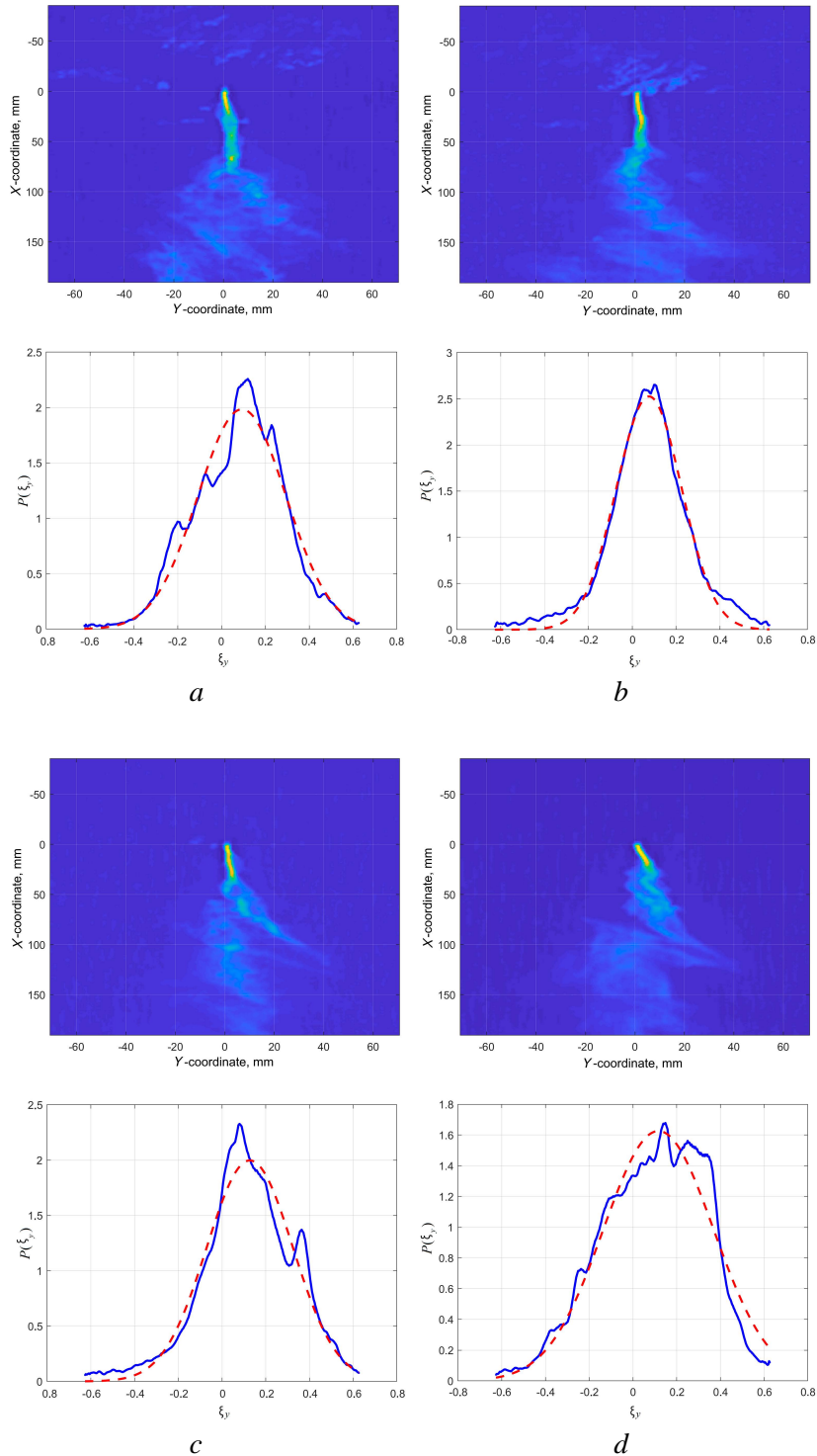


**Fig. 11.** Accumulation of the beam image for 0.1 s (nine frames) in the crest area (in the frame interval 2618–2653 in Fig. 9) (*top*); corresponding slope distributions (*bottom*): *a* – frames 2618–2626; *b* – 2627–2635; *c* – 2636–2644; *d* – 2645–2653

## Discussion

The proposed light “skirt” method allows the measurement of the distribution of capillary-wave slopes over surface areas of  $10 \times 10$  cm in 0.1 s. Unlike traditional methods, it does not require complex calibration, can be used in a wide range of illumination conditions, including during the daytime, and does not involve placing structural elements in the water.

The obtained values of capillary-slope dispersion on crests (0.0256) and in troughs (0.0049) are consistent with the physical understanding that capillary-wave generation is more intense on the crests of long waves due to increased effective wind speed and nonlinear effects. These data also qualitatively correspond to the results obtained in [24, 25] for the modulation of short waves by long waves.

The correctness of the laser “skirt” method has been verified by comparing the total slope dispersion obtained by accumulating frames over several periods of the energy-containing waves with the dispersion calculated using the Cox–Munk formulas [10]. In the present experiment (22 February 2025 at 02:55 Moscow time), when accumulating 1500 frames (16.7 s), the measured total slope dispersion was  $\sigma_y^2 = 0.018 \pm 0.003$ . The dispersion according to the Cox–Munk model for a wind speed of 7.4 m/s and a direction differing by  $12^\circ$  from the  $Y$  axis was  $\sigma_c^2 = 0.017 \pm 0.002$ . The agreement within the error limits of the compared methods confirms the reliability of the proposed method.

The MTF estimate (6.6) is preliminary, as it is based on a single processed measurement. To establish the dependences of the MTF on meteorological parameters and physical processes, further systematic measurements are required. Nevertheless, the given example demonstrates the capabilities of the proposed method for studying capillary waves on small areas of the sea surface.

## Conclusions

In this work, a new method for the operational measurement of the slope distribution of capillary waves on the sea surface is proposed. The method is based on analyzing the brightness distribution of laser “skirts” formed when a laser beam is incident on the sea surface and on recording the scattered radiation from the side of the incidence point using a video camera. It is shown that the width of the “skirt” is proportional to the magnitude of the slopes, and that the intensity distribution in the cross-section of the “skirt” allows the calculation of the slope probability density. The method enables the recording of capillary waves with an amplitude of  $30 \mu\text{m}$  from a distance of 5–8 m and allows measurements in 0.01 s over surface areas of  $10 \times 10$  cm. The advantage of the proposed method is the ability to perform measurements in a wide range of illumination conditions, including during the daytime. Measurements are possible even from a single frame or from several frames.

Under field conditions, the method was applied to study the capillary structure on crests and in troughs of gravity waves. It was found that the dispersion of capillary slopes in troughs is significantly lower than that on crests, which is consistent with known data on the modulation of short waves by long waves. The obtained results demonstrate the potential of the method for studying capillary waves in the open sea.

## REFERENCES

1. Kwoh, D.S.W. and Lake, B.M., 1986. Microwave Scattering from Short Gravity Waves. In: O. M. Phillips and K. Hasselmann, eds., 1986. *Wave Dynamics and Radio Probing of the Ocean Surface*. Boston, MA: Springer, pp. 443-447. [https://doi.org/10.1007/978-1-4684-8980-4\\_30](https://doi.org/10.1007/978-1-4684-8980-4_30)
2. Ermakov, S.A., Sergievskaya, I.A., Dobrokhotoy, V.A. and Lazareva, T.N., 2022. Wave Tank Study of Steep Gravity-Capillary Waves and Their Role in Ka-Band Radar Backscatter. *IEEE Transactions on Geoscience and Remote Sensing*, 60, 4202812. <https://doi.org/10.1109/TGRS.2021.3086627>
3. Ermakov, S.A., Kapustin, I.A. and Sergievskaya, I.A., 2012. On Peculiarities of Scattering of Microwave Radar Signals by Breaking Gravity-Capillary Waves. *Radiophysics and Quantum Electronics*, 55(7), pp. 453-461. <https://doi.org/10.1007/s11141-012-9381-1>
4. Rozenberg, A., Matusov, P. and Melville, W.K., 1998. Polarized Microwave Scattering by Surface Water Waves and Turbulence. In: IEEE, 1998. *IGARSS'98. Sensing and Managing the Environment. 1998 IEEE International Geoscience and Remote Sensing: Symposium Proceedings*. Seattle, WA, USA: IEEE. Vol. 4, pp. 2273-2275. <https://doi.org/10.1109/IGARSS.1998.703810>
5. Falcon, E. and Mordant, N., 2022. Experiments in Surface Gravity-Capillary Wave Turbulence. *Annual Review of Fluid Mechanics*, 54(1), pp. 1-25. <http://dx.doi.org/10.1146/annurev-fluid-021021-102043>
6. Bobb, L.C., Ferguson, G. and Rankin, M., 1979. Capillary Wave Measurements. *Applied Optics*, 18(8), pp. 1167-1171. <https://doi.org/10.1364/AO.18.001167>
7. Lukaschuk, S., Nazarenko, S., McLelland, S. and Denissenko, P., 2009. Gravity Wave Turbulence in Wave Tanks: Space and Time Statistics. *Physical Review Letters*, 103(4), 044501. <https://doi.org/10.1103/PhysRevLett.103.044501>
8. Soman, S.S. and Singh, S.K., 2025. Study of Evolving Young Wind Waves under Steady Wind Forcing. *Journal of Offshore Mechanics and Arctic Engineering*, 147(5), 051201. <https://doi.org/10.1115/1.4067551>
9. Xu, C. and Perlin, M., 2023. Parasitic Waves and Micro-Breaking on Highly Nonlinear Gravity-Capillary Waves in a Convergent Channel. *Journal of Fluid Mechanics*, 962, A46. <https://doi.org/10.1017/jfm.2023.322>
10. Cox, C. and Munk, W., 1954. Measurement of the Roughness of the Sea Surface from Photographs of the Sun's Glitter. *Journal of the Optical Society of America*, 44(11), pp. 838-850. <https://doi.org/10.1364/JOSA.44.000838>
11. Bréon, F.M. and Henriot, N., 2006. Spaceborne Observations of Ocean Glint Reflectance and Modeling of Wave Slope Distributions. *Journal of Geophysical Research: Oceans*, 111(C6), C06005. <https://doi.org/10.1029/2005JC003343>
12. Yurovskaya, M.V., Kudryavtsev, V.N., Shirokov, A.S. and Nadolya, I.Yu., 2018. Field Measurements of the Sea Surface Wave Spectrum from Photos of Sun glitter Taken from Drone. *Sovremennye Problemy Distantionnogo Zondirovaniya Zemli iz Kosmosa*, 15(1), pp. 245-257. <https://doi.org/10.21046/2070-7401-2018-15-1-245-257> (in Russian).
13. Kosnik, M.V. and Dulov, V.A., 2011. Extraction of Short Wind Wave Spectra from Stereo Images of the Sea Surface. *Measurement Science and Technology*, 22(1), 015504. <https://doi.org/10.1088/0957-0233/22/1/015504>
14. Yurovskaya, M.V., Dulov, V.A., Chapron, B. and Kudryavtsev, V.N., 2013. Directional Short Wind Wave Spectra Derived from the Sea Surface Photography. *Journal of Geophysical Research: Oceans*, 118(9), pp. 4380-4394. <https://doi.org/10.1002/jgrc.20296>

15. Laxague, N.J.M., Zappa, C.J., LeBel, D.A. and Banner, M.L., 2018. Spectral Characteristics of Gravity-Capillary Waves, with Connections to Wave Growth and Microbreaking. *Journal of Geophysical Research: Oceans*, 123(7), pp. 4576-4592. <https://doi.org/10.1029/2018JC013859>
16. Zappa, C.J., Banner, M.L., Schultz, H., Corrada-Emmanuel, A., Wolff, L.B. and Yalcin, J., 2008. Retrieval of Short Ocean Wave Slope Using Polarimetric Imaging. *Measurement Science and Technology*, 19(5), 055503. <https://doi.org/10.1088/0957-0233/19/5/055503>
17. Zappa, C.J., Banner, M.L., Schultz, H., Gemmrich, J.R., Morison, R.P., LeBel, D.A. and Dickey, T., 2012. An Overview of Sea State Conditions and Air-Sea Fluxes during RaDyO. *Journal of Geophysical Research: Oceans*, 117(C7), C00H19. <https://doi.org/10.1029/2011JC007336>
18. Hughes, B.A., Grant, H.L. and Chappell, R.W., 1977. A Fast Response Surface-Wave Slope Meter and Measured Wind-Wave Moments. *Deep Sea Research*, 24(12), pp. 1211-1223. [https://doi.org/10.1016/0146-6291\(77\)90524-0](https://doi.org/10.1016/0146-6291(77)90524-0)
19. Sterlyadkin, V.V., Kulikovskiy, K.V., Kuzmin, A.V., Sharkov, E.A. and Likhacheva, M.V., 2021. Scanning Laser Wave Recorder with Registration of “Instantaneous” Sea Surface Profiles. *Journal of Atmospheric and Oceanic Technology*, 38(8), pp. 1415-1424. <https://doi.org/10.1175/JTECH-D-21-0036.1>
20. Sterlyadkin, V.V., Kulikovskii, K.V. and Badulin, S.I., 2024. Field Measurements of Sea Surface Shape and One-Dimensional Spatial Wave Spectrum. *Sovremennye Problemy Distantionnogo Zondirovaniya Zemli iz Kosmosa*, 21(1), pp. 270-285. <https://doi.org/10.21046/2070-7401-2024-21-1-270-285> (in Russian).
21. Sterlyadkin, V.V. and Kulikovskiy, K.V., 2022. Measurement of Capillary Waves with a Laser Wave Recorder. *Russian Technological Journal*, 10(5), pp. 100-110. <https://doi.org/10.32362/2500-316X-2022-10-5-100-110> (in Russian).
22. Sterlyadkin, V.V., 2024. The Problem of Reconstructing the Profile of the Sea Surface from the Video Image of Laser Beams. *Oceanology*, 64(3), pp. 342-352. <https://doi.org/10.1134/S0001437024700024>
23. Sterlyadkin, V.V., Kulikovskiy, K.V. and Zadernovskiy, A.A., 2025. Measurement of Capillary Oscillations of the Sea Surface. *Oceanology*, 65(2), pp. 201-211. <https://doi.org/10.1134/S0001437024701030>
24. Dulov, V.A., Korinenko, A.E., Kudryavtsev, V.N. and Malinovsky, V.V., 2021. Modulation of Wind-Wave Breaking by Long Surface Waves. *Remote Sensing*, 13(14), 2825. <https://doi.org/10.3390/rs13142825>
25. Donelan, M.A., Haus, B.K., Plant, W.J. and Troianowski, O., 2010. Modulation of Short Wind Waves by Long Waves. *Journal of Geophysical Research: Oceans*, 115(C10), C10003. <https://doi.org/10.1029/2009JC005794>

Submitted 17.08.2025; approved after review 12.10.2025;  
accepted for publication 28.01.2026.

*About the authors:*

**Viktor V. Sterlyadkin**, Professor at the Department of Physics and Technical Mechanics, MIREA - Russian Technological University (78 Prospekt Vernadskogo, Moscow, 119454, Russian Federation), DSc. (Phys.-Math.), **ORCID ID: 0000-0002-1832-8608**, **Web of Science ResearcherID: D-7125-2017**, **Scopus Author ID: 6505940691**, **SPIN-code: 8368-0889**, [sterlyadkin@mail.ru](mailto:sterlyadkin@mail.ru)

**Konstantin V. Kulikovskiy**, Associate Professor at the Department of Physics and Technical Mechanics, MIREA - Russian Technological University (78 Prospekt Vernadskogo, Moscow, 119454, Russian Federation), CSc. (Tech.), **ORCID ID: 0000-0001-9296-6424**, **Scopus Author ID: 57223241696**, **Web of Science ResearcherID: D-7125-2017**, **SPIN-code: 8368-0889**, [constantinkk@mail.ru](mailto:constantinkk@mail.ru)

**Maria V. Likhacheva**, Senior Lecturer at the Department of Physics and Technical Mechanics, MIREA - Russian Technological University (78 Prospekt Vernadskogo, Moscow, 119454, Russian Federation), **ORCID ID: 0009-0007-6021-080X**, **Scopus Author ID: 23005642200**, **Web of Science ResearcherID: OBN-9238-2025**, **SPIN-code: 4548-9098**, [likhacheva.m@gmail.com](mailto:likhacheva.m@gmail.com)

*Contribution of the co-authors:*

**Viktor V. Sterlyadkin** – development of a theoretical basis for measuring sea wave slopes by analyzing the shape of a laser beam below its point of impact on the surface; participation in experiments and video image processing

**Konstantin V. Kulikovsky** – development of equipment and a video recording system; participation in field measurements

**Maria V. Likhacheva** – participation in conducting field measurements and processing video images

*The authors have read and approved the final manuscript.*

*The authors declare that they have no conflict of interest.*